ISSN 1024-8560, Atmospheric and Oceanic Optics, 2019, Vol. 32, No. 1, pp. 72–79. © Pleiades Publishing, Ltd., 2019.
Russian Text © O.Yu. Antokhina, P.N. Antokhin, V.G. Arshinova, M.Yu. Arshinov, B.D. Belan, S.B. Belan, D.K. Davydov, N.V. Dudorova, G.A. Ivlev, A.V. Kozlov, T.M. Rasskazchikova, D.E. Savkin, D.V. Simonenkov, T.K. Sklyadneva, G.N. Tolmachev, A.V. Fofonov, 2018, published in Optika Atmosfery i Okeana.

OPTICAL MODELS AND DATABASES

Study of Air Composition in Different Air Masses

O. Yu. Antokhina[a, *], P. N. Antokhin[a, **], V. G. Arshinova[a], M. Yu. Arshinov[a], B. D. Belan[a], S. B. Belan[a], D. K. Davydov[a], N. V. Dudorova[a], G. A. Ivlev[a], A. V. Kozlov[a], T. M. Rasskazchikova[a], D. E. Savkin[a], D. V. Simonenkov[a], T. K. Sklyadneva[a], G. N. Tolmachev[a], and A. V. Fofonov[a]

[a] *V.E. Zuev Institute of Atmospheric Optics, Siberian Branch, Russian Academy of Sciences, Tomsk, 634055 Russia*

**e-mail: michael@iao.ru*

***e-mail: bbd@iao.ru*

Received May 21, 2018; revised May 21, 2018; accepted June 22, 2018

Abstract—Data of multiyear monitoring at the TOR station are used to calculate the average concentrations of gas and aerosol constituents in different air masses in the region of Tomsk. It is shown that CO_2 and CH_4 are characterized by a decrease in concentrations in going from an Arctic to a tropical air mass. Ozone shows the opposite pattern: the largest concentrations are recorded in the tropical air mass and the smallest concentrations in the Arctic air mass. Such gases as CO and SO_2 show distributions more complex in character.

Keywords: atmosphere, aerosol, air mass, gas, concentration, content, composition

DOI: 10.1134/S1024856019010020

INTRODUCTION

S.P. Khromov was one of the first to point out an optical inhomogeneity in air masses. In his work [1], he showed that the integrated (over spectrum and atmospheric depth) turbidity factor is almost the same inside a single air mass and drastically changes in either going from one to another air mass or after a change in air mass type at the measurement site. The analysis in [2–4] showed that the turbidity factor is determined by air composition, which, in turn, depends on the character of synoptic processes. This was also noted elsewhere [5–9]. It is noteworthy that the transport direction and prehistory of air masses influence the air composition [10–13].

Elements of the atmospheric general circulation influence both the general level of admixture concentrations in air [14, 15] and the content of individual gases: ozone [16–18], carbon dioxide [6, 7], nitrogen oxides [8], and aerosol particles of different sizes [19–21]. However, despite the fact that the synoptic processes have an appreciable effect, the air composition is determined by the region of formation of the air mass and by the presence of sources and sinks for a particular admixture [22–25]. As a result, an air mass as a whole turns out to be inhomogeneous not only optically, but also in composition [26]. Of course, this is fulfilled provided that there are no large-scale admixture sources such as forest fires [27–31].

Also, the air composition in the observation region behaves in a specific way after a change of air masses. Change occurs not simply in an abrupt manner, but rather via quite a complex mechanism, determined by dynamic processes in the zone of frontal divides, solubility of gases in atmospheric precipitation, and the hydrophilic or hydrophobic character of aerosol particles [32–37].

The above-listed features of distribution of air composition inside air masses and when passing from one air mass to another suggest that these differences can be very significant. Therefore, the problem formulated in the present paper is to determine the concentrations of gas and aerosol constituents in different air masses in the region of Tomsk, where we for a long time have monitored the air composition, as well as its specific features during changes from one air mass type to another.

STUDY REGION AND ANALYSIS METHODS

Studies were performed based on measurements at the TOR station, which has been operating since December 1992 [38] till the present. In this paper, we analyzed the changes in trace atmospheric gases (TAGs) CO_2, CH_4, CO, SO_2, and O_3 and the chemical composition of aerosol. TAGs were measured using the following instruments: a Picarro G2301-m gas analyzer for carbon dioxide (in the range from 0 to 1000 ppm, with error <0.2 ppm) and methane (in the range from 0 to 20 ppm, with error <0.0015 ppm); an OPTEK K-100 electrochemical gas analyzer for carbon oxide (in the range from 0 to 50 mg/m^3, with error ±20%); a Teledyne API 100E fluorescent ultraviolet gas analyzer for sulfur dioxide (in the range from 0 to 20 ppm, with error ±0.5%); an OPTEK 3.02-P chemiluminescent

Table 1. Average concentrations and standard deviations of TAGs in different air masses near Tomsk

Air mass type	CO_2, ppm	*N*	CH_4, ppb	*N*	CO, ppb	*N*	SO_2, ppb	*N*	O_3, μg/m^3	*N*
Arctic	428 ± 26	1647	2069 ± 153	1647	327 ± 267	4424	11.4 ± 5.2	4424	27 ± 16	4424
Midlatitude	418 ± 25	1126	2022 ± 114	1126	361 ± 278	7038	10.6 ± 5.5	7045	40 ± 24	7046
Subtropical	417 ± 20	675	2011 ± 2	675	330 ± 171	5196	11.9 ± 5.8	5241	50 ± 23	5243
Tropical	418 ± 10	85	2003 ± 52	85	355 ± 295	671	12.5 ± 4.8	687	55 ± 20	687

N is the number of cases.

gas analyzer for ozone (in the range from 0 to 500 μg/m^3, with error ±20%).

The measurements of CO_2, CH_4, CO, SO_2, and O_3 concentrations in different air masses and during frontal passage were analyzed for 2015 and 2016. The air mass type was identified using synoptic charts.

The aerosol chemical composition was analyzed using data from aircraft sensing that has been performed since July 1997 to the present over Karakan pine forest southwest of Novosibirsk. Samples were collected on AFA-KhA and AFA-KhP filters. Atmospheric aerosol samples were chemically analyzed in the Department of Analytic Chemistry at Tomsk State University. The detection limits were 0.1–0.6 μg/filter for ions and 0.01–0.02 μg/filter for elements.

AIR COMPOSITION IN DIFFERENT AIR MASSES

The results of determining the average concentrations of TAGs in the main air mass types and the corresponding average deviations are presented in Table 1.

From Table 1 it follows that the CO_2 concentration is maximal in the Arctic air mass and smaller in warmer air masses, with a minimum in the subtropical air mass. The differences in the average concentrations between Arctic and midlatitude air masses are confident at the 0.001 level. The differences in the average concentrations among midlatitude, subtropical, and tropical air masses do not even attain the minimal 0.05 significance level. This pattern reflects the distribution of carbon dioxide sources and sinks over the regions where air masses form [39].

This same gradient, directed from cold to warm air, is also observed for methane (Table 1). The largest (2069 ppb) CH_4 concentration is recorded in the Arctic air mass, and the smallest (2003 ppb) CH_4 concentration is recorded in the tropical air mass. The differences in the average concentrations between the Arctic and midlatitude (between the midlatitude and subtropical) masses are significant at the 0.001 (0.01) confidence level. The differences in the concentrations between the subtropical and tropical air masses are unreliable, possibly, like for CO_2, due to the small frequency of occurrence (in only 85 cases) of tropical masses. This CH_4 distribution is most probably due to the sources located in the Arctic Ocean [40–42] and Vasyugan bogs, from the surface of which methane is emitted even more strongly than from the Arctic source [43].

Despite the fact that the globally averaged CO concentration decreases [44, 45], high CO concentrations were recorded in the region under study in all air masses (Table 1). The carbon monoxide concentration is the largest (361 ppb) in the midlatitude air mass, somewhat smaller (355 ppb) in the tropical air mass, and the smallest (327 ppb) in the Arctic air mass, where neither natural nor anthropogenic sources exist [26]. This CO distribution seems to be due to a high-power industrial source in Western Europe, from which, as shown in [46], CO is transported in midlatitudes to the territory of Siberia. A larger CO concentration in the tropical mass is due to the effect of a powerful source in these latitudes [47, 48]. It is noteworthy that the differences in the average concentrations between the Arctic and midlatitude masses, and between the midlatitude and subtropical masses, are significant at the 0.001 confidence level. The differences in the average concentrations between subtropical and tropical masses are significant at the 0.01 confidence level.

Efforts of the worldwide community directed to reduce anthropogenic sulfur dioxide emissions have led to a considerable decrease in the background SO_2 concentration in many regions on the globe [49–51]. This can also be seen from Table 1, where the SO_2 concentration varies from 10.6 ppb in the midlatitude air mass to 12.5 ppb in the tropical air mass, with the difference in the average concentrations among all air masses being significant at the 0.001 confidence level. Nonetheless, the minor absolute differences in SO_2 concentrations between air masses complicate their interpretation.

Ozone is characterized by a gradient opposite to that for CO_2 and CH_4 (see Table 1). The smallest (27 μg/m^3) average ozone concentration is observed in the Arctic air mass, and the largest (55 μm/m^3) concentration is observed in the tropical air mass. As for SO_2, the differences in the average concentrations among all air masses are significant at the 0.001 confidence level. On the one hand, this reflects the influx of precursor gases and UV-B radiation that determine the concentration of tropospheric ozone [52]. On the

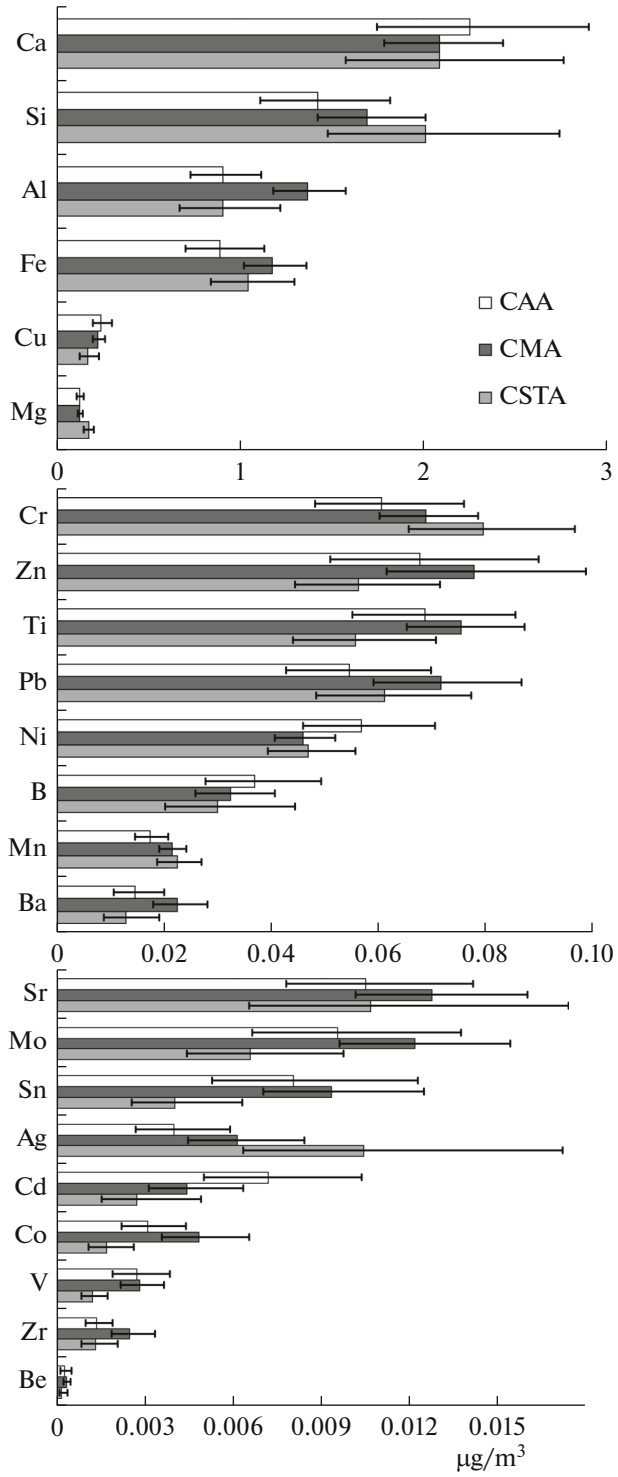

Fig. 1. Geometric mean concentrations of elements in the region of Karakan pine forest in different types of air masses (here, CAA is continental Arctic air, CMA is continental midlatitude air, and CSTA is continental subtropical and tropical air); error bars indicate the confidence intervals at the $P = 0.95$ level, calculated from standard deviations, also evaluated for logarithms of concentrations.

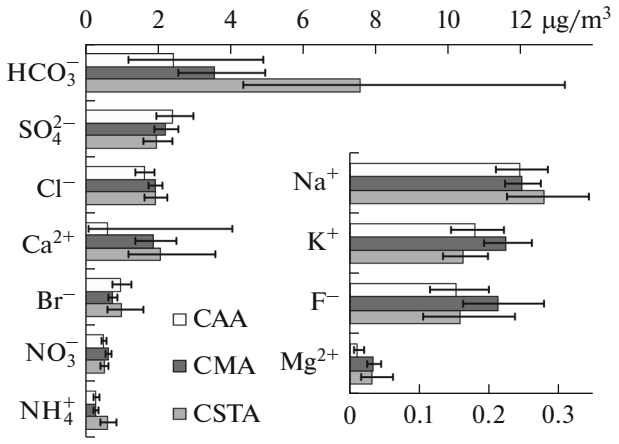

Fig. 2. Same as in Fig. 1, but for ion concentrations.

other hand, the recently found nonlinear dependence of the O_3 production rate on increasing air temperature [53] should also show up.

The distribution of concentrations of chemical constituents obeys the lognormal law; therefore, the average values and standard deviations were calculated for logarithms of concentrations, for which we then calculated the confidence interval at the $P = 0.95$ level. That is, the averages (or, more specifically, the geometric averages) and boundaries of confidence intervals (Figs. 1 and 2) are antilogarithms of the values obtained. The numbers of the used samples are presented in Table 2.

The analysis of aerosol chemical composition for different air mass types makes it possible to draw preliminary conclusions on latitudinal patterns of origin of separate elements and inorganic ions, classifying them by this feature into the corresponding groups (Figs. 1 and 2).

Silicon, chromium, manganese, silver (Fig. 1), and bicarbonate anions are clearly southern in origin (Fig. 2); however, the last constituent has a low statistical reliability, despite the fact that HCO_3^- concentration exhibits the strongest peak. Chlorine and sodium ions tend to belong to this same group, probably because they are long-range transported together with marine aerosol (Fig. 2).

The microelements copper, boron, cadmium, nickel (Fig. 1), and sulfate anion (Fig. 2) are directly correlated with arctic Air masses. Evidently, they are all anthropogenic in origin, confirming the high accumulation ability of Arctic air.

Midlatitude air is associated with most representative group of elements (aluminum, iron, zinc, titanium, lead, barium, strontium, molybdenum, tin, cobalt, vanadium, and zirconium) and ions (potassium, fluoride, and nitrate) in tropospheric aerosol in the south of Western Siberia (Fig. 1). Evidently, the midlatitude mass is local or zonal in origin; therefore,

Table 2. Number of samples for each air mass and chemical element used to calculate the average values and confidence interval

Chemical element	Air mass type		
	subtropical	midlatitude	arctic
Mg	154	511	238
Cu	170	495	231
Fe	158	488	235
Al	170	551	266
Si	162	518	237
Ca	158	527	250
Ba	125	306	150
Mn	151	467	207
B	35	149	81
Ni	143	426	198
Pb	136	403	185
Ti	138	449	202
Zn	91	159	94
Cr	159	426	204
Be	46	131	53
Zr	58	140	68
V	91	232	127
Co	91	202	109
Cd	42	114	45
Ag	24	81	49
Sn	103	245	115
Mo	111	268	141
Sr	24	98	50
Sb	0	2	8
NH_4^+	67	161	88
NO_3^-	135	433	215
Br^-	28	164	54
Ca^{2+}	8	32	8
Cl^-	157	516	253
SO_4^{2-}	117	370	207
HCO_3^-	7	43	13
Mg^{2+}	6	30	9
F^-	13	46	11
K^+	127	415	217
Na^+	139	435	228

taking into consideration the dominant fluxes, we can predict the main contribution from western regions, i.e., the Urals and Northern Kazakhstan, as well as from Kuzbass and, in a number of cases, from central regions of the Eastern Siberian plateau.

SPECIFIC FEATURES OF VARIATIONS IN AIR COMPOSITION DURING CHANGE IN AIR MASSES

Weather fronts are complex structures accompanied by changes in clouds and precipitation in pre- and post-frontal areas, rapid changes in temperature, and wind strengthening and convergence (measurements were performed at a single point at one-hour intervals); therefore, for each case we used the data of hourly measurements 5 h before and 5 h after front passage. During the period under study (2015–2016), 167 cold, 145 warm, and 128 occluded fronts passed over Tomsk.

During the passage of a warm front, the CO_2 concentration decreases, reaches a minimum behind the frontal line, and then somewhat increases (Fig. 3a). The CO_2 concentration is found to behave in a similar way during cold front passage (Fig. 3b) but reaches a minimum 1 hour before the front passage.

During the passage of a warm front, the changes in CH_4 concentration show a pronounced decrease while changing from the cold to the warm air mass (Fig. 3c). The methane concentration curve is multimodal in the cold front, with the two main minima occurring 3 h before and 3 h after the front passage (Fig. 3d).

In addition to the general decrease in concentration during a change from cold to warm air masses (Fig. 3e), and the increase during passage from warm to cold air masses (Fig. 3f), the CO concentration behavior is more complex than of CO_2 and CH_4 concentrations.

Although having minor amplitudes in both warm and cold frontal zones (Figs. 3g and 3h), the variations in SO_2 concentration are more complex in the frontal zone.

In order to mitigate the effects of seasonal and diurnal variations in gas concentrations during the study of O_3 concentration, data on gas concentrations were normalized to their values during front passage [35]. Therefore, results in Fig. 3 are in relative units.

During the passage of a warm front, the CO_2 concentration decreases to the minimum behind the frontal line and then somewhat increases (Fig. 3a). The CO_2 concentration is found to behave in a similar way during cold front passage (Fig. 3b), but reaches a minimum 1 hour before the front passage.

During the passage of a worm front, the O_3 concentration is characterized by an increase during a change from cold to warm air masses (Fig. 3i). In the frontal zone, the concentration increases by about 30%. From Fig. 3j it can be seen that, during cold front passage, the O_3 concentration rapidly decreases when changing from cold to warm air masses, with the change in concentration being ~25%. Behind the front, the O_3 concentration stabilizes and remains almost unchanged.

We will not give an interpretation for our data, because, as was shown some time ago [1], each front is a complex structure with many specific features. Our

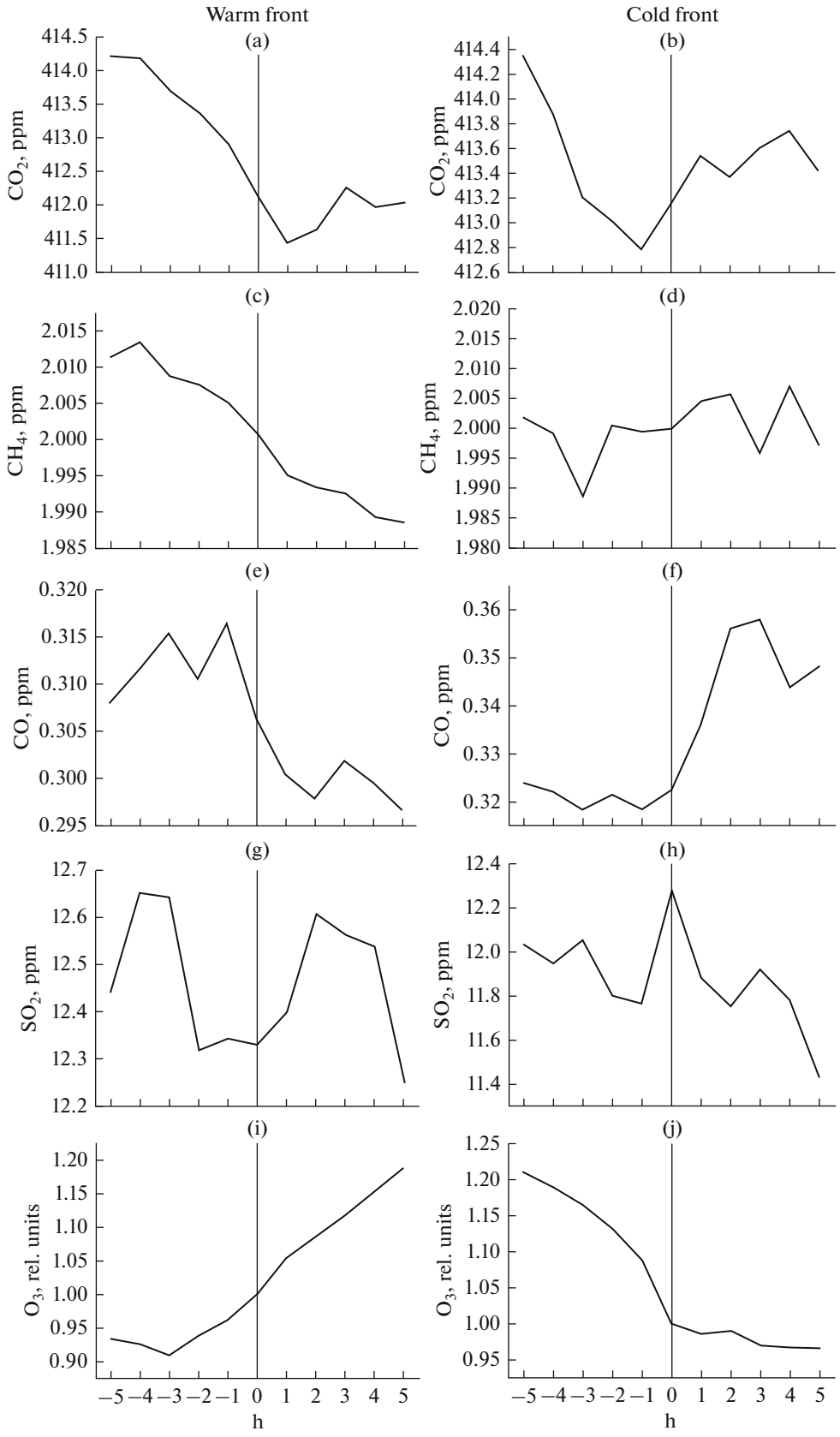

Fig. 3. Changes in TAG concentrations during passages of warm (a, c, e, g, i) and cold (b, d, f, h, j) fronts over Tomsk. Negative (positive) half-axis is for pre- (post-) front passage times.

purpose was to estimate the general tendency of variations and verify the estimates of gas concentrations in different air masses.

CONCLUSIONS

From our results, we can conclude that each air mass has a specific air composition, with salient features identified with confidence in a number of cases, in terms of both atmospheric gases and the chemical composition of aerosol particles.

The gas concentrations change nonlinearly when changing from one to another air mass. It is noteworthy that the direction of the gradient depends on the air composition in cold and warm air masses.

ACKNOWLEDGMENTS

This work was supported by the Russian Science Foundation (grant no. 17-17-01095).

REFERENCES

1. S. P. Khromov, *Foundations of Synoptic Meteorology* (Gidrometizdat, Leningrad, 1948) [in Russian].
2. V. E. Zuev, B. D. Belan, and G. O. Zadde, *The Optical Weather* (Nauka, Novosibirsk, 1990) [in Russian].
3. B. D. Belan, G. O. Zadde, A. I. Kuskov, and T. M. Rasskazchikova, "Spectral transmittance of the atmosphere of basic synoptic objects," Atmos. Ocean. Opt. **7** (9), 640–645 (1994).
4. B. D. Belan, G. O. Zadde, and A. I. Kuskov, "Long-period variations of the spectral transmittance of the atmosphere," Atmos. Ocean. Opt. **7** (10), 721–724 (1994).
5. R. M. Law, L. P. Steele, P. B. Krummel, and W. Zahorowski, "Synoptic variations in atmospheric CO_2 at Cape Grim: A model intercomparison," Tellus B **62** (5), 810–820 (2010).
6. M. Klavins and V. Rodinov, "Influence of large-scale atmospheric circulation on climate in Latvia," Boreal Environ. Res. **15** (6), 533–543 (2010).
7. J. Zhang, L. Wu, G. Huang, and M. Notaro, "Relationships between large-scale circulation patterns and carbon dioxide exchange by a deciduous forest," J. Geophys. Res. **116** (D4), 1–13 (2011).
8. R. J. Pope, N. H. Savage, M. P. Chipperfield, S. R. Arnold, and T. J. Osborn, "The influence of synoptic weather regimes on UK air quality: Analysis of satellite column NO_2," Atmos. Sci. Lett. **15** (3), 211–217 (2014).
9. L. Pace, L. Boccacci, M. Casilli, P. Di Carlo, and S. Fattorini, "Correlations between weather conditions and airborne pollen concentration and diversity in a Mediterranean high-altitude site disclose unexpected temporal patterns," Aerobiology **34** (1), 75–87 (2018).
10. A. M. Zvyagintsev, G. Kakadzhanova, and O. A. Tarasova, "Influence of air mass transport directions on the seasonal variations of concentrations of minor gas atmospheric components in Europe," Rus. Meteorol. Hydrol., No. 7, 441–448 (2010).
11. D. Coumou, J. Lehmann, and J. Beckmann, "The weakening summer circulation in the Northern Hemisphere mid-latitudes," Science **348** (6232), 324–327 (2015).
12. I. A. Perez, M. L. Sanchez, M. A. Garcia, and N. Pardo, "An experimental relationship between airflow and carbon dioxide concentrations at a rural site," Sci. Total Environ. **533**, 432–438 (2015).
13. J. Fu, B. Wang, Y. Chen, and Q. Ma, "The influence of continental air masses on the aerosols and nutrients deposition over the western North Pacific," Atmos. Environ. **172**, 1–11 (2018).
14. H. Flocas, A. Kelessis, C. Helmis, M. Petrakakis, M. Zoumakis, and K. Pappas, "Synoptic and local scale atmospheric circulation associated with air pollution episodes in an urban Mediterranean area," Theor. Appl. Climatol. **95** (3-4), 265–277 (2009).
15. S. A. Sitnov, I. I. Mokhov, G. I. Gorchakov, and A. V. Dzhola, "Smoke haze over the European part of Russia in the summer of 2016: A link to wildfires in Siberia and atmospheric circulation anomalies," Rus. Meteorol. Hydrol., No. 8, S. 518–528 (2017).
16. U. Dayan and I. Levy, "Relationship between synoptic-scale atmospheric circulation and ozone concentrations over Israel," J. Geophys. Res. **107** (D24), 1–12 (2002).
17. J. E. Diem, M. A. Hursey, I. R. Morris, A. C. Murray, and R. A. Rodriguez, "Upper-level atmospheric circulation Patterns and ground-level ozone in the Atlanta Metropolitan area," J. Appl. Meteorol. Climatol. **49** (11), 2185–2196 (2010).
18. Y. Zhang, H. Mao, A. Ding, D. Zhou, and C. Fu, "Impact of synoptic weather patterns on spatio-temporal variation in surface O_3 levels in Hong Kong during 1999–2011," Atmos. Environ. **73**, 41–50 (2013).
19. J. de Arellano and N. P. M. Lipzig, "The impact of weather and atmospheric circulation on O_3 and PM_{10} levels at a rural mid-latitude site," Atmos. Chem. Phys. **9** (8), 2695–2714 (2009).
20. K. G. T. Dharshana, S. Kravtsov, and J. D. W. Kahl, "Relationship between synoptic weather disturbances and particulate matter air pollution over the United States," J. Geophys. Res. **115** (D24), 1–16 (2010).
21. E. Flaounas, V. Kotroni, K. Lagouvardos, S. Kazadzis, A. Gkikas, and N. Hatzianastassiou, "Cyclone contribution to dust transport over the Mediterranean region," Atmos. Sci. Lett. **16** (4), 473–478 (2015).
22. G. R. MeGregor and D. Bamzelis, "Synoptic typing and its application to the investigation of weather air pollution relationships, Birmingham, United Kingdom," Theor. Appl. Climatol. **51** (4), 223–236 (1995).
23. Z. L. Fleming, P. S. Monks, and A. J. Manning, "Review: Untangling the influence of air-mass history in interpreting observed atmospheric composition," Atmos. Res. **104-105** (1), 1–39 (2012).
24. C. Orbe, M. Holzer, L. M. Polvani, and D. Waugh, "Air-mass origin as a diagnostic of tropospheric transport," J. Geophys. Res.: Atmos. **118** (3), 1459–1470 (2013).
25. S. Freitag, A. D. Clarke, S. G. Howell, V. N. Kapustin, T. Campos, V. L. Brekhovskikh, and J. Zhou, "Combining airborne gas and aerosol measurements with

HYSPLIT: A visualization tool for simultaneous evaluation of air mass history and back trajectory consistency," Atmos. Meas. Tech. **7** (1), 107–128 (2014).

26. P. N. Antokhin, V. G. Arshinova, M. Yu. Arshinov, B. D. Belan, S. B. Belan, D. K. Davydov, G. A. Ivlev, A. V. Kozlov, F. Nedelek, J. -D. Paris, T. M. Rasskazchikova, D. E. Savkin, D. V. Simonenkov, T. K. Sklyadneva, G. N. Tolmachev, and A. V. Fofonov, "Large-scale studies of gaseous and aerosol composition of air over Siberia," Opt. Atmos. Okeana **27** (3), 232–239 (2014).
27. N. F. Elanskii, I. I. Mokhov, I. B. Belikov, E. V. Berezina, A. S. Elokhov, V. A. Ivanov, N. V. Pankratova, O. V. Postylyakov, A. N. Safronov, A. I. Skorokhod, and R. A. Shumskii, "Gaseous admixtures in the atmosphere over Moscow during the 2010 summer," Izv., Atmos. Ocean. Phys. **47** (6), 672–681 (2011).
28. A. M. Zvyagintsev, O. B. Blyum, A. A. Glazkova, S. N. Kotel'nikov, I. N. Kuznetsova, V. A. Lapchenko, E. A. Lezina, E. A. Miller, V. A. Milyaev, A. P. Popikov, E. G. Semutnikova, O. A. Tarasova, and I. Yu. Shalygina, "Air pollution over European Russia and Ukraine under the hot summer conditions of 2010," Izv., Atmos. Ocean. Phys. **47** (6), 699–707.
29. E. V. Fokeeva, A. N. Safronov, V. S. Rakitin, L. N. Yurganov, E. I. Grechko, and R. A. Shumskii, "Investigation of the 2010 July-August fires impact on carbon monoxide atmospheric pollution in Moscow and its outskirts, estimating of emissions," Izv., Atmos. Ocean. Phys. **47** (6), 682–698 (2011).
30. F. V. Kashin, V. N. Aref'ev, N. I. Sizov, R. M. Akimenko, and L. B. Upenek, "Background component of carbon oxide concentrations in the surface air (Obninsk monitoring station)," Izv., Atmos. Ocean. Phys. **52** (3), 247–252 (2016).
31. P. N. Antokhin, V. G. Arshinova, M. Yu. Arshinov, B. D. Belan, S. B. Belan, D. K. Davydov, G. A. Ivlev, A. V. Fofonov, A. V. Kozlov, J.-D. Paris, P. Nedelec, T. M. Rasskazchikova, D. E. Savkin, D. V. Simonenkov, T. K. Sklyadneva, and G. N. Tolmachev, "Distribution of trace gases and aerosols in the troposphere over Siberia during wildfires of summer 2012," J. Geophys. Res.: Atmos. **123** (4), 2285–2297 (2018).
32. T. R. Lee, S. F. J. De Wekker, A. E. Andrews, J. Kofler, and J. Williams, "Carbon dioxide variability during cold front passages and fair weather days at a forested mountaintop site," Atmos. Environ. **46** (1), 405–416 (2012).
33. X. M. Hu, P. M. Klein, M. Xue, A. Shapiro, and A. Nallapareddy, "Enhanced vertical mixing associated with a nocturnal cold front passage and its impact on near-surface temperature and ozone concentration," J. Geophys. Res.: Atmos. **118** (7), 2714–2728 (2013).
34. G. M. Scott and R. D. Diab, "Forecasting air pollution potential: A synoptic climatological approach," J. Air Waste Manag. Assoc. **50** (10), 1831–1842 (2000).
35. V. G. Arshinova, B. D. Belan, T. M. Rasskazchikova, A. N. Rogov, and G. N. Tolmachev, "Variation of the ozone concentration in the ground atmospheric layer by the passage of atmospheric fronts," Atmos. Ocean. Opt. **8** (4), 625–631 (1995).
36. V. G. Arshinova, B. D. Belan, E. V. Vorontsova, G. O. Zadde, T. M. Rasskazchikova, O. I. Sem'yanova, and T. K. Sklyadneva, "Dynamics of aerosol variations during passage of atmospheric fronts," Atmos. Ocean. Opt. **10** (7), 507–511 (1997).
37. P. N. Antokhin, M. Yu. Arshinov, V. G. Arshinova, B. D. Belan, D. K. Davydov, T. M. Rasskazchikova, A. V. Fofonov, G. Inoue, T. Machida, Ko. Shimoyama, and Sh. Sh. Maksutov, "CO_2 concentration variation above the West Siberia area in different seasons during passes of atmospheric fronts," Opt. Atmos. Okeana **26** (1), 24–31 (2013).
38. M. Yu. Arshinov, B. D. Belan, V. V. Zuev, V. E. Zuev, V. K. Kovalevskii, A. V. Ligotskii, V. E. Meleshkin, M. V. Panchenko, E. V. Pokrovskii, A. N. Rogov, D. V. Simonenkov, and G. N. Tolmachev, "TOR-station for monitoring of atmospheric parameters," Atmos. Ocean. Opt. **7** (8), 580–584 (1994).
39. C. Le Quere, R. N. Andrew, P. Friedlingstein, S. Sitch, J. Pongratz, A. C. Manning, J. I. Korsbakken, G. P. Peters, J. G. Canadell, R. B. Jackson, T. A. Boden, P. P. Tans, O. D. Andrews, V. K. Arora, D. C. E. Bakker, L. Barbero, M. Becker, R. A. Betts, L. Bopp, C. Chevallier, L. P. Chini, P. Ciais, C. E. Cosca, J. Cross, K. Currie, T. Gasser, I. Harris, J. Hauck, V. Haverd, R. A. Houghton, C. W. Hunt, G. Hurtt, T. Ilyina, A. K. Jain, E. Kato, M. Kautz, R. F. Keeling, K. K. Goldewijk, A. Kortzinger, P. Landschutzer, N. Lefevre, A. Lenton, S. Lienert, I. Lima, D. Lombardozzi, N. Metzl, F. Millero, P. M. S. Monteiro, D. R. Munro, J. E. M. S. Nabel, S. Nakaoka, Y. Nojiri, X. A. Padin, A. Peregon, B. Pfeil, D. Pierrot, B. Poulter, G. Rehder, J. Reimer, C. Rodenbeck, J. Schwinger, R. Seferian, I. Skjelvan, B. D. Stocker, H. Tian, B. Tilbrook, F. N. Tubiello, I. T. van der Laan-Luijkx, G. R. van der Werf, S. van Heuven, N. Viovy, N. Vuichard, A. P. Walker, A. J. Watson, A. J. Wiltshire, S. Zaehle, and D. Zhu, "Global carbon budget 2017," Earth Syst. Sci. Data **10** (1), 405–448 (2018).
40. N. Shakhova, I. Semiletov, A. Salyuk, V. Yusupov, D. Kosmach, and O. Gustafsson, "Extensive methane venting to the atmosphere from sediments of the East Siberian Arctic Shelf," Science **327** (5970), 1246–1250 (2010).
41. I. P. Semiletov, N. E. Shakhova, V. I. Sergienko, I. I. Pipko, and O. V. Dudarev, "On carbon transport and fate in the East Siberian Arctic land-shelf-atmosphere system," Environ. Res. Lett. **7** (1), 13 (2012).
42. S. Hartery, R. Commane, J. Lindaas, C. Sweeney, J. Henderson, M. Mountain, N. Steiner, K. McDonald, S. J. Dinardo, C. E. Miller, S. C. Wofsy, and R. Y.-W. Chang, "Estimating regional-scale methane flux and budgets using CARVE aircraft measurements over Alaska," Atmos. Chem. Phys. **18** (1), 185–202 (2018).
43. O. Yu. Antokhina, P. N. Antokhin, V. G. Arshinova, M. Yu. Arshinov, B. D. Belan, S. B. Belan, D. K. Davydov, G. A. Ivlev, A. V. Kozlov, P. Nédélec, J.-D. Paris, T. M. Rasskazchikova, D. E. Savkin, D. V. Simonenkov, T. K. Sklyadneva, G. N. Tolmachev, and A. V. Fofonov, "Vertical distributions of gaseous and

aerosol admixtures in air over the Russian Arctic," Atmos. Ocean. Opt. **31** (3), 300–310 (2018).

44. S. A. Strode and S. Pawson, "Detection of carbon monoxide trends in the presence of interannual variability," J. Geophys. Res.: Atmos. **118** (21), 12257–12273 (2013).
45. Y. Zhou, H. Mao, K. Demerjian, C. Hogrefe, and J. Liu, "Regional and hemispheric influences on temporal variability in baseline carbon monoxide and ozone over the Northeast US," Atmos. Environ. **164**, 309–324 (2017).
46. Yu. A. Shtabkin, K. B. Moiseenko, A. I. Skorokhod, A. V. Vasileva, and M. Khaimann, "Sources of and variations in tropospheric CO in Central Siberia: Numerical experiments and observations at the Zotino Tall Tower Observatory," Izv., Atmos. Ocean. Phys. **52** (1), 45–56 (2016).
47. L. El Amraoui, J.-L. Attie, P. Ricaud, W. A. Lahoz, A. Piacentini, V.-H. Peuch, J. X. Warner, R. Abida, J. Barre, and R. Zbinden, "Tropospheric CO vertical profiles deduced from total columns using data assimilation: Methodology and validation," Atmos. Meas. Tech. **7** (9), 3035–3057 (2014).
48. K. Park, L. K. Emmons, Z. Wang, and J. E. Mak, "Joint application of concentration and δ18O to investigate the global atmospheric CO budget," Atmosphere **6** (5), 547–578 (2015).
49. V. Vestreng, G. Myhre, H. Fagerli, S. Reis, and L. Tarrason, "Twenty-five years of continuous sulphur dioxide emission reduction in Europe," Atmos. Chem. Phys. **7** (13), 3663–3681 (2007).
50. S. J. Smith, J. van Aardenne, Z. Klimont, R. J. Andres, A. Volke, and S. D. Arias, "Anthropogenic sulfur dioxide emissions: 1850–2005," Atmos. Chem. Phys. **11** (3), 1101–1116 (2011).
51. S. Henschel, X. Querol, R. Atkinson, M. Pandolfi, A. Zeka, A. Le Tertre, A. Analitis, K. Katsouyanni, O. Chanel, M. Pascal, C. Bouland, D. Haluza, S. Medina, and P. G. Goodman, "Ambient air SO_2 patterns in 6 European cities," Atmos. Environ. **79**, 236–247 (2013).
52. B. D. Belan, *Tropospheric Ozone* (Publishing House of IAO SB RAS, Tomsk, 2010) [in Russian].
53. B. D. Belan, D. E. Savkin, and G. N. Tolmachev, "Air—temperature dependence of the ozone generation rate in the surface air layer, Atmos. Ocean. Opt. **31** (2), 187–196 (2018).

Translated by O. Bazhenov